Diurnal Variation in Nonstructural Carbohydrate Storage in Trees: Remobilization and Vertical Mixing[1]

Aude Tixier,[a,2] Jessica Orozco,[a] Adele Amico Roxas,[a] J. Mason Earles,[b] and Maciej A. Zwieniecki[a,2,3]

[a]Department of Plant Sciences, University of California, Davis, California 95616
[b]Yale School of Forestry and Environmental Studies, New Haven, Connecticut 06511

ORCID IDs: 0000-0002-7712-4795 (A.T.); 0000-0002-2023-9735 (A.A.R.); 0000-0002-8345-9671 (J.M.E.).

Nonstructural carbohydrate (NSC) storage plays a critical role in tree function and survival, but understanding and predicting local NSC storage dynamics is challenging because NSC storage pools are dispersed throughout the complex architecture of trees and continuously exchange carbon between source and sink organs at different time scales. To address these knowledge gaps, characterization and understanding of NSC diel variation are necessary. Here, we analyzed diurnal NSC dynamics in the overall architecture of almond (*Prunus dulcis*) trees. We also analyzed the allocation of newly assimilated carbon using isotopic labeling. We show that both components of NSC (i.e. soluble carbohydrates and starch) are highly dynamic at the diurnal time scale and that these trends are influenced by tissue type, age, and/or position within the canopy. In leaves, starch reserves can be depleted completely during the night, while woody tissue starch levels may vary by more than 50% over a daily cycle. Recently assimilated carbon showed a dispersed downward allocation across the entire tree. NSC diurnal fluctuations within the tree's structure in combination with dispersed carbon allocation patterns provide evidence for the presence of vertical mixing and suggest that the xylem acts as a secondary NSC redistribution pathway.

Nonstructural carbohydrates (NSC; soluble carbohydrates and starch) fulfill distinct pivotal functions in plants such as transport, energy metabolism, osmosis, and serving as the building blocks for growth and structure. NSC allocation toward these functions has to be balanced with storage in order to buffer supply and demand asynchronies on different temporal scales. During periods of low to no photosynthetic activity, such as night, severe water stress, and dormancy, plants are entirely dependent on NSC storage (Stitt and Zeeman, 2012; Charrier et al., 2015; Hartmann and Trumbore, 2016). While NSC reserves are critical to plant resilience, their allocation patterns, fluxes, age composition, and turnover remain elusive, especially in the context of long-lived plants. The perennial habit of trees and their delayed maturity imply that they have to maintain both short-term and long-term NSC reserves to ensure survival and fitness (Hartmann and Trumbore, 2016). The continuous maintenance of positive local reserves pivotally buffers periods of stress during the growing season. Accumulated reserves also are crucial for winter dormancy and spring development (Hoch et al., 2003; Sala et al., 2012; Richardson et al., 2013; Muhr et al., 2016). Understanding and predicting NSC dynamics is challenging, not only because of these multiple demands at different time scales but also because dispersed storage sites within the complex architecture of trees continually buffer exchanges between source and sink organs. While there are large seasonal fluctuations in tree trunk NSC content, it also has been shown that stored starch may reside for over 50 years in central trunk wood (Hartmann and Trumbore, 2016; Muhr et al., 2016). The presence of such long-term pools coincides with short-term pools at the trunk periphery that are more or less mobilized depending on the severity of stress/demand (Keel et al., 2007; Richardson et al., 2015). The dynamics of local reserves also are complex because they involve the mixing of both newly formed and decades-old NSC (Keel et al., 2006, 2007; Richardson et al., 2015). Indeed, newly assimilated carbon has been shown to pass through existing mobile NSC pools before being transferred to structural sinks. While the identification of these mixing processes highlights the complexity of NSC dynamics in trees, the time scale and underlying mechanisms remain elusive. Increasing evidence shows that starch formation/degradation and NSC partitioning are environmentally responsive. These processes also may occur on a much shorter (e.g. diurnal) time scale than was expected previously (Stitt and Zeeman, 2012; Wada et al., 2017).

Diel variation of NSC reserves has been studied intensively in herbaceous species; however, it remains

[1] This work was supported by the Almond Board of California and the California Walnut Board.

[2] Senior authors.

[3] Author for contact: aude.tixier@yahoo.fr

The author responsible for distribution of materials integral to the findings presented in this article in accordance with the policy described in the Instructions for Authors (www.plantphysiol.org) is: Maciej A. Zwieniecki (mzwienie@ucdavis.edu).

This work was conceptualized and written by A.T., J.O., J.M.E., and M.A.Z.; the field experiment was performed by A.T., J.O., A.A.R., and M.A.Z.; analysis was performed by A.T., J.O., and A.A.R.; A.T. analyzed the data, performed the statistical analysis, and prepared the figures for publication.

www.plantphysiol.org/cgi/doi/10.1104/pp.18.00923

overlooked within the complex architecture of perennial woody plants (Zeeman et al., 2002; Bucci et al., 2003; Graf and Smith, 2011; Pyl et al., 2012; Stitt and Zeeman, 2012; Streb and Zeeman, 2012; Richardson et al., 2015; Woodruff et al., 2015). Some insights may be drawn from herbaceous species. For example, Arabidopsis (*Arabidopsis thaliana*) leaves store a portion of photoassimilates as starch during the day and remobilize and export it at night for respiration and growth. However, the differences in life habits, architecture, and size of storage tissues suggest that observations in herbaceous annual species are unlikely to represent trees (Loescher et al., 1990; Witt and Sauter, 1994; Hoch et al., 2003; Nogués et al., 2006; Regier et al., 2010; Hartmann and Trumbore, 2016). Larger woody plants demand NSC in organs often separated by tens of meters, which requires a fine-tuned and complex balance between NSC redistribution, mixing processes, maintenance of positive local storage, and long-term NSC pools (Lacointe et al., 2004; Richardson et al., 2013, 2015; Dietze et al., 2014; Sperling et al., 2017; Tixier et al., 2017). Additionally, the largest fraction of NSC storage occurs in xylem parenchyma cells, which are absent in the herbaceous Arabidopsis (Chaffey et al., 2002).

Detailed analyses of diurnal NSC dynamics within mature trees that include high spatial (specific tissue, canopy location, and age) and temporal (hours) resolution are lacking in the literature, despite their importance in the establishment of a proper basis and time scale for the study of NSC mixing and redistribution processes. A complete picture of NSC diurnal dynamics in different tissues, positions, and ages is necessary to build a mechanistic understanding of overall tree NSC storage dynamics. Unraveling short-term diurnal trends is crucial for addressing questions regarding abiotic stress responses and long-term climate change resilience. Besides, knowing the existence of such dynamics and their magnitude for different tissues of interest is a prerequisite for the determination of tissue sample collection time (Sala et al., 2012; Charrier et al., 2013; Hartmann et al., 2013; Woodruff et al., 2015). If the diurnal dynamics of NSC in trees represents a balance between assimilation and utilization, as in their herbaceous counterparts, their dendritic structure implies a significant contribution of transport and redistribution processes to NSC turnover. The use of isotopes provides a convenient way to track newly assimilated NSC and their fluxes to dispersed NSC pools. Previous studies using isotopes were performed mostly on seedlings or saplings. Thus, the spatial pattern of new assimilate allocation and storage replenishment, as well as the extent of vertical carbohydrate mixing, remain largely unexplored in larger trees (Hansen, 1967; Norris et al., 2012). Working on saplings allows for a cost-effective detection of small amounts of ^{13}C at the whole organism level, with repeated observations for statistical purposes. However, pulse labeling on full-grown trees is required to understand the allocation and transport pathways of new assimilates throughout dispersed storage pools with high spatial and temporal resolution (Lacointe et al., 2004; Keel et al., 2007).

We present the first study of diurnal NSC dynamics in almond trees (*Prunus dulcis*) in combination with short-term temporal dynamics of newly assimilated carbon using isotope labeling. We hypothesize that starch concentration in woody tissues exhibits strong diurnal variations as a result of soluble carbohydrate (SC) influx and efflux together with the concomitant interconversion of starch and sugars. These fluxes and interconversion processes could lead to the mixing of both new and old sugars and result in the formation of amalgamated starch granules that are later remobilized. Furthermore, we hypothesize that vertical mixing processes are correlated with diurnal cycles. To test these hypotheses, we studied diurnal NSC dynamics and the allocation of new assimilates at high temporal and spatial resolution in the overall tree architecture, which showed downward transport, dispersed allocation, and vertical mixing. As sugars have been reported to accumulate in xylem sap, we analyzed the diurnal variations of xylem sap sugar concentration to evaluate the potential of xylem for sugar transport and its involvement in vertical mixing (Secchi and Zwieniecki, 2011).

RESULTS

Diurnal Dynamics of Local NSC

We observed a significant effect of time of day on local NSC concentration in every tissue studied except for the trunk central region (trunk C) samples. The comparison of total NSC concentrations between two consecutive days at 13:00 did not show significant differences (Student's t test, $\alpha < 0.05$), providing assurance that, over a short period of time (days), NSC do not accumulate significantly and vary in a periodic pattern. Starch concentrations showed a systematic effect of time of day in all but the trunk C and bark tissues, whereas SC concentrations were constant in leaves, branches, trunk C, and coarse roots (Table 1; Supplemental Fig. S1). Based on the maximum likelihood method, sinusoidal functions generated the best-fitting trends for the diurnal variation of NSC concentrations observed within each tissue (Figs. 1–3). However, all sinusoidal trends in the studied tissues were asynchronous (phase shifts).

Leaf starch accumulated during the day, reaching a maximum of 7 ± 1.6 mg g^{-1} dry weight at 13:00, which remained constant until 17:00. Overnight, starch concentration decreased to 0.1 ± 0.1 mg g^{-1} at 5:00 (Fig. 1B). SC represented 90% to 100% of the total leaf NSC, with an average concentration of 72.3 ± 1.4 mg g^{-1} dry weight (Fig. 1A). NSC concentration in the wood storage tissues showed diurnal trends, with patterns specific to position in canopy and/or age (Table 1; Figs. 2 and 3). Wood in twigs showed the highest level of SC, with a maximum concentration at

Table 1. *Effect of time on SC and starch concentrations in leaf, twig, branch, trunk (trunk peripheral region [trunk P] and trunk C), root, and sap*

P values obtained from an ANOVA performed on a nonlinear mixed-effects model are shown. Minimum and maximum values (mean ± SE) and time of NSC diurnal trends were calculated on five trees.Starch was not detected in sap (no signal (ns).

Diurnal Trend	Leaf	Twig	Branch	Trunk P	Trunk C	Coarse Root	Fine Root	Sap
SC *P* values	0.1555	0.0024	0.2605	<0.0001	0.0820	0.4220	0.0005	0.0001
Starch *P* values	<0.0001	<0.0001	<0.0001	<0.0001	0.3721	0.0189	<0.0001	ns
SC_{max}	79.9 ± 1.3	78.3 ± 12.2	34.2 ± 0.9	38.3 ± 2.1	33.6 ± 4.4	125.7 ± 15.7	113.4 ± 9.2	1.7 ± 0.3
SC_{min}	63.9 ± 4.0	41.2 ± 5.5	26.5 ± 2.0	24.4 ± 3.1	22.5 ± 2.6	94.6 ± 8.5	84.2 ± 11.6	0.6 ± 0.3
Time SC_{max}	13:00	5:00	17:00	17:00	17:00	13:00	17:00	5:00
Time SC_{min}	5:00	21:00	9:00	5:00	9:00	9:00	5:00	21:00
$Starch_{max}$	7.0 ± 1.6	64.5 ± 11.5	28.9 ± 2.0	20.0 ± 2.9	10.9 ± 2.9	113.9 ± 17.2	65.6 ± 6.1	ns
$Starch_{min}$	0.1 ± 0.1	33.0 ± 2.1	14.8 ± 3.5	12.3 ± 0.9	3.7 ± 0.5	47.5 ± 18.2	27.1 ± 4.5	ns
Time $starch_{max}$	13:00	5:00	17:00	1:00	1:00	17:00	1:00	ns
Time $starch_{min}$	5:00	17:00	5:00	9:00	5:00	21:00	17:00	ns

5:00 of 78.3 ± 12.2 mg g^{-1} dry weight and a minimum at 21:00 of 41.2 ± 5.5 mg g^{-1} dry weight and the greatest magnitude of change with a 50% SC pool change during the day (Fig. 2A). Branch wood showed lower concentrations of SC (44 ± 2.4 mg g^{-1} dry weight), which remained constant through the day (Fig. 2B). Trunk P showed a sinusoidal antiphase to the twig wood trend, with accumulation of SC during the day reaching a maximum of 38.3 ± 2.1 mg g^{-1} dry weight and depletion during the night to a minimum concentration of 24.4 ± 3.1 mg g^{-1} dry weight at 5:00 (Fig. 2C). Congruent to SC dynamics, aboveground young tissues with smaller storage capacities had a greater magnitude of starch fluctuation and concentration compared with older and larger woody tissues. For example, twigs showed a 51% change from 64.5 ± 11.5 mg g^{-1} dry weight at 5:00 to 33 ± 2.1 mg g^{-1} dry weight at 17:00 (Fig. 2D). In addition, diurnal starch level patterns in leaves and twig wood were inverted similarly. Starch showed nocturnal accumulation in the twigs and trunk, although not synchronous, while accumulation occurred during the day for branches (Fig. 2, D–F). Branches reached minimum starch concentration at dawn (14.8 ± 3.5 mg g^{-1} dry weight) and maximum concentration at the end of the day, with 28.9 ± 2 mg g^{-1} dry weight at 17:00. Starch diurnal concentration in the trunk P reached a maximum of 20 ± 2.9 mg g^{-1} dry weight at 1:00 and a minimum of 12.3 ± 0.9 mg g^{-1} dry weight at midday.

As sink organs, roots had the highest concentrations of NSC. We observed asynchronous diurnal trends of starch concentrations in fine and coarse roots, ranging from 27.1 ± 4.5 to 65.6 ± 6.1 mg g^{-1} dry weight (58% variation) in fine roots and from 47.5 ± 18.2 to 113.9 ± 17.2 mg g^{-1} dry weight (58% variation) in coarse roots (Fig. 3, E and F). High and constant concentrations of SC were observed in coarse roots through the day (108.9 ± 4.8 mg g^{-1} dry weight) while they oscillated diurnally in fine roots (Fig. 3, B and C).

Starch concentrations were constant in the bark of twigs, with 19.7 ± 18.2 mg g^{-1} dry weight (Supplemental Fig. S1), but time of day had a significant effect on bark SC concentration, with values ranging from 69.7 ± 6.8 to 90.8 ± 6.1 mg g^{-1} dry weight. While NSC trends in twig bark were asynchronized with the neighboring wood, the diurnal trend of SC concentration in the xylem sap was in phase with the NSC (both SC and starch) trends observed in twig wood (Fig. 2, A and D). During the night, when xylem sap flow decreased to a nearly null value, xylem sap SC concentration increased, reaching a maximum of 1.7 ± 0.3 mg mL^{-1} at 5:00 before sunrise (Fig. 4). After sunrise, SC concentration dropped to 0.8 ± 0.1 mg mL^{-1} and remained low until sunset.

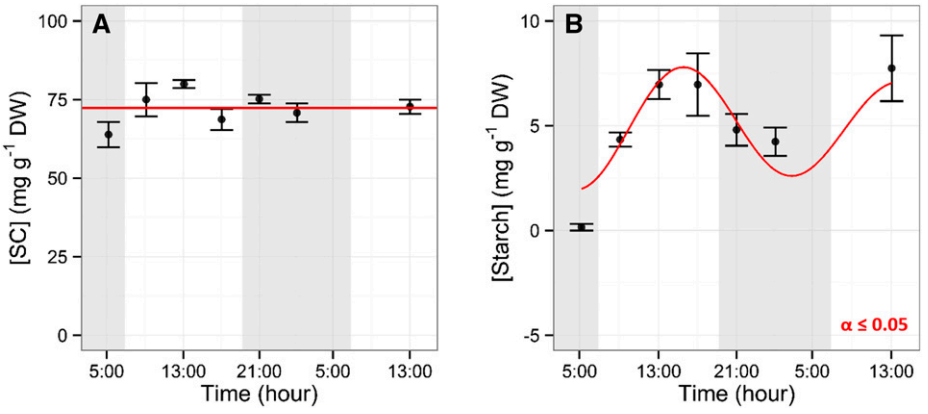

Figure 1. Diurnal NSC trends in leaves. Leaf diurnal dynamics of SC (A) and starch (B) concentrations are shown. Leaves were collected every 4 h. Data points represent mean values from five trees. Error bars represent SE. Shaded areas represent nighttime. A significant effect of time of day was observed for starch ($P \leq 0.05$, using a nonlinear mixed-effects model). Red lines represent mixed-effects model predictions. DW, Dry weight.

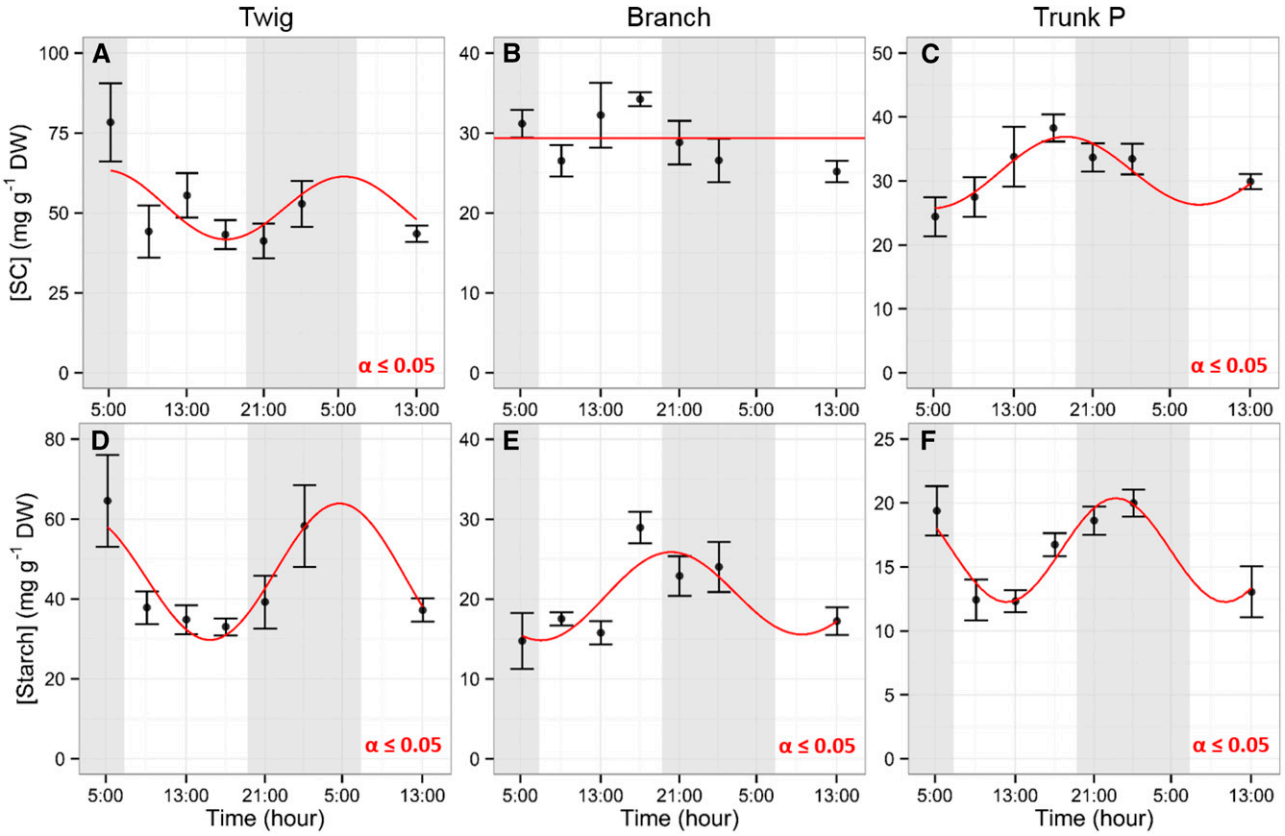

Figure 2. Diurnal NSC trends in wood. Diurnal dynamics of SC (A–C) and starch (D–F) in wood of twig (A and D), branch (B and E), and trunk P (C and F) are shown. Samples were collected every 4 h. Data points represent mean values from five trees. Error bars represent SE. Shaded areas represent nighttime. A significant effect of time of day was observed for each analysis except SC in branch ($P \leq 0.05$, using a nonlinear mixed-effects model). Red lines represent mixed-effects model predictions. DW, Dry weight.

Based on the estimated biomass from the L-Almond model, total NSC content in the tree ranged from 3.55 ± 0.56 kg at 9:00 to 4.73 ± 0.75 kg at 17:00, with increasing NSC storage during the daytime followed by a decrease during the nighttime (Supplemental Fig. S2). Roots represented the biggest storage pool, with on average 44.2% ± 1.4% of the total NSC due to their high NSC concentrations and sizable biomass. Conversely, twigs accounted for only 2.7% ± 0.3% of the total storage due to their small biomass contribution. Trunk and branches represented 10.4% ± 0.3% and 42.7% ± 1.3%, respectively.

Temporal Analysis of the Redistribution of Newly Assimilated Carbon Using Enriched $^{13}CO_2$

Assimilation of the $^{13}CO_2$ in leaves by photosynthesis was successful and resulted in a strong increase of atomic percent excess (APE) of ^{13}C in treated leaves on all three trees (Fig. 5). APE levels were variable between the trees and reached 0.33% to 0.55%. In the three trees, elevated levels of ^{13}C in leaves remained relatively constant over the first night and then decreased steadily during the first day, reaching 0.2% to 0.08% (Fig. 5, A–C). The values and rate of APE changes were specific and slightly different in each branch studied, but leaves seemed to export/dilute most of the newly acquired labeled carbon within 20 to 24 h following exposure (Fig. 5). Noticeably, the first-day dilution of ^{13}C APE was followed by an increase of ^{13}C in leaf tissue, which occurred at different times for each tree (6:00 the following day and 11:00 the day after for tree 1, 23:00 and 5:00 on tree 2, and 23:00 two days after for tree 3). Although the three trees showed different temporal patterns and the statistical significance of APE could not be estimated in our design, this counterintuitive increase suggested the return of ^{13}C in the form of NSC to mature (nongrowing) leaves. Similar increases of ^{13}C in leaf tissue also were observed in tree saplings each morning after the day of the labeling event (Supplemental Fig. S3).

^{13}C APE also increased, to a lesser extent than in leaves, in twig bark and wood tissues after the labeling event, with maximum APE values reaching 0.09% and 0.16% for wood and bark, respectively (Fig. 5, D–F). ^{13}C accumulation occurred simultaneously in bark and leaves at 17:00 after the pulse event, whereas ^{13}C excess maximum was observed in the wood following a delay of 6 h at 23:00. Similar to leaves, the increase in APE was followed by a decrease. A daytime increase during the

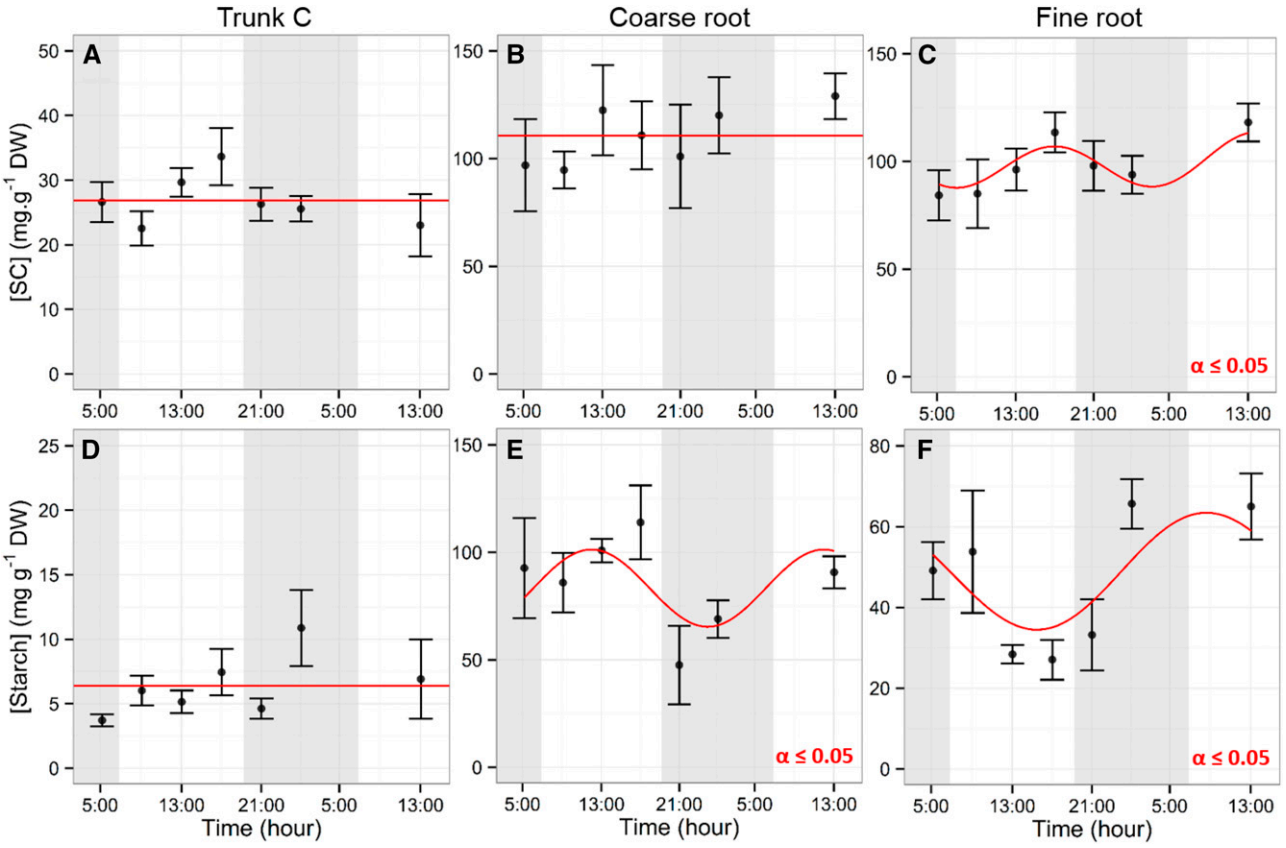

Figure 3. Diurnal NSC trends in wood and roots. Diurnal dynamics of SC (A–C) and starch (D–F) in trunk C (A and D), coarse roots (B and E), and fine roots (C and F) are shown. Samples were collected every 4 h. Shaded areas represent nighttime. Data points represent mean values from five trees. Error bars represent SE. A significant effect of time of day was observed for starch concentrations in coarse and fine roots ($P \leq 0.05$, using a nonlinear mixed-effects model). Red lines represent mixed-effects model predictions. DW, Dry weight.

following days was noticed in all three trees tested. In branches, ^{13}C maximum excess was detected later than in leaves and twigs (Fig. 5, G–I). Except for tree 2, no detection of excess ^{13}C was observed in trunk or roots. For each tissue, an increase in ^{13}C APE following the labeling event was tailed by a decrease, which was followed subsequently by an increase (Fig. 5). Yet, these temporal trends were not synchronous between the three trees studied.

Pulse $^{13}CO_2$ labeling experiments on small potted trees allowed us to analyze the allocation of new assimilates over a short time scale. On the first day after pulse labeling, APE increased significantly in leaves from the bagged branch containing $^{13}CO_2$, while control leaves remained at the initial level (Fig. 6). Two days later (day 3), the APE levels in the ^{13}C-exposed leaves decreased significantly and concurrently with increases in the roots, trunk, and twigs, while control twigs remained at the initial level.

DISCUSSION

In this study, we found evidence that tree NSC storage is highly dynamic at the diurnal time scale, shedding light on the importance of the dark phase. To our knowledge, this is the first report showing that diurnal NSC trends are not only tissue specific but that their timing and magnitude also are influenced by age and/or position within the canopy. Diurnal variation in the starch concentration of woody tissues can provide a time frame and a potential explanatory mechanism for the mixing of old and new NSC during the growing season. Yet, the potential seasonal variability of NSC diurnal trends due to endogenous regulation should be addressed in the future to fully comprehend these mechanisms. In our study, sampling for NSC diurnal trends and ^{13}C allocation patterns was performed at different times during the summer. Future studies should test the significance of the proposed xylem redistribution path and evaluate the putative influence of seasonal rhythms. Furthermore, we show that NSC allocation to storage on short time scales is dispersed and occurs with a downward movement, from branches to trunk to roots, with the likely downward path occurring in the phloem. SC accumulation in xylem sap during the night, and the counterintuitive observations of ^{13}C patterns in leaves and storage tissues, raise interesting questions about NSC redistribution pathways

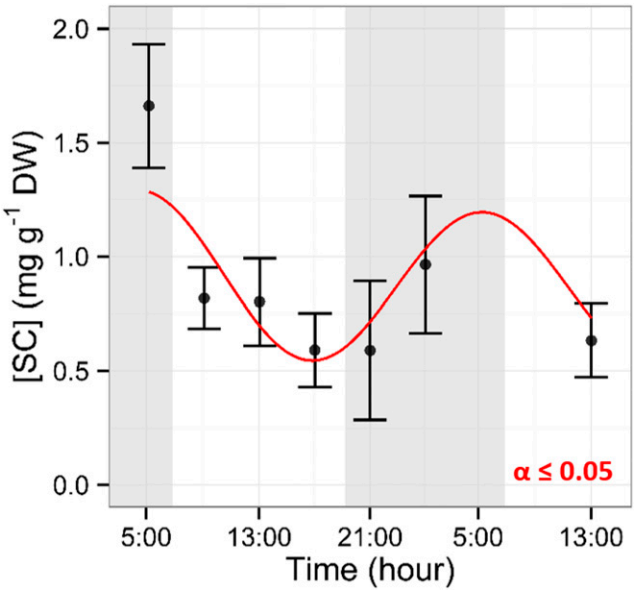

Figure 4. Diurnal dynamics of SC in xylem sap. Samples were collected every 4 h. Shaded areas represent nighttime. Data points represent mean values from five trees. Error bars represent SE. A significant effect of time of day was observed ($P \leq 0.05$, using a nonlinear mixed-effects model). The red line represents the mixed-effects model predictions. DW, Dry weight.

and the xylem's possible role as a secondary redistribution path for sugars in the overall tree architecture.

Tree Storage Mixing and Transport at the Diurnal Scale

We found and report here that there are significant cyclic diurnal variations in woody tissue starch concentrations throughout the entire tree, including the trunk and roots, with oscillations from maximum to minimum values following a sinusoidal trend. Roots are shown to be a main storage compartment, with substantial diel fluctuations that strongly influence the overall tree NSC variation (Fig. 3; Supplemental Fig. S2). In aboveground tissue, the magnitude of NSC variation decreases with tissue age, being highest for twigs, smallest for the branches and trunk, while still highly variable in roots (Figs. 2 and 3). The observation that storage size reduces diurnal variability is in line with the observed ^{13}C APE dynamics in twigs, branches, and trunk (Fig. 5; Supplemental Fig. S2). The largest variation of APE was observed in twigs, where small amounts of NSC could not mask the influx of newly assimilated $^{13}CO_2$. Recent work on radiocarbon (^{14}C) dating of NSC pools in trees has shown evidence that younger tissues tend to present strong mixing of NSC while older tissues tend to show more limited mixing (Richardson et al., 2015). We provide evidence that, indeed, large diurnal variations of NSC occur in young organs and tissues (twigs, branches, and trunk P areas; Fig. 2). Interestingly, these large variations in NSC concentrations are observed mainly for starch. Cumulatively over the growing season, diurnal starch and sugar interconversions are probably involved in the mixing processes of NSC storage pools observed in numerous species (Keel et al., 2007; Muhr et al., 2016). The smaller magnitude of variations observed in SC supports the idea that sugar status is maintained to prevent energy deprivation or osmotic imbalance (Stitt and Zeeman, 2012). Additionally, the smaller magnitude of NSC concentration variation in older and larger aboveground organs also suggests that a less mobile pool is maintained in these tissues, which probably buffers long-term stress responses and supplies seasonal demands (Sala et al., 2012; Richardson et al., 2013). Interestingly, coarse roots showed higher diurnal variations and may represent a key mobile storage pool (Loescher et al., 1990).

Daily maximum and minimum SC and starch concentrations diverged from the whole-tree trend depending on tissue age and/or location (Figs. 1–3). The observed temporal variation of NSC in almond tree leaves is in accordance with that of herbaceous plants (Stitt and Zeeman, 2012). Daytime starch accumulation as a product of photosynthesis is followed by a decrease during the night as a result of respiration and sugar translocation, reaching a nearly null value at dawn (Fig. 1). However, while starch represented 90% of leaf NSC in Arabidopsis, it only contributed to 10% of the total NSC in almond (Fig. 1). Interestingly, starch diurnal trends observed earlier in the year exhibited a phasic pattern, but dawn values were slightly higher (3.3 ± 0.7 mg g^{-1}), suggesting that tree leaf starch turnover might be shifted during the growing season (Supplemental Fig. S4). A similar decrease in leaf starch concentration during the growing season also has been observed in juniper (*Juniperus monosperma*) and pine (*Pinus edulis*; Woodruff et al., 2015). Diurnal maximums and minimums of NSC levels for woody tissues did not exhibit synchronized patterns of starch accumulation/diminution. In fact, twig wood showed the exact antiphase trend to leaves (Fig. 2) while trunk and branch tissue seemed to reach a maximum concentration prior to the twig, seemingly counter to their distance from the leaves. Both types of roots also did not show synchrony in their diurnal trends of starch concentrations (Fig. 3). The large magnitude of asynchronous NSC fluctuation in individual storage compartments in comparison with the lower magnitude of changes (especially at night) of whole-tree NSC storage suggests the presence of remobilization and retranslocation of NSC across the tree structure prior to being used locally for metabolism or growth (Supplemental Fig. S2; Keel et al., 2006). Our findings on the allocation and dispersal of newly fixed carbon throughout the entire tree architecture support the idea of vertical mixing between woody tissues (Fig. 5, D–I) and advocate for a shift from models showing simple lagged downward NSC accumulation after photosynthesis. We expect that future modeling efforts could provide a mechanistic understanding of these complex storage/transport dynamics.

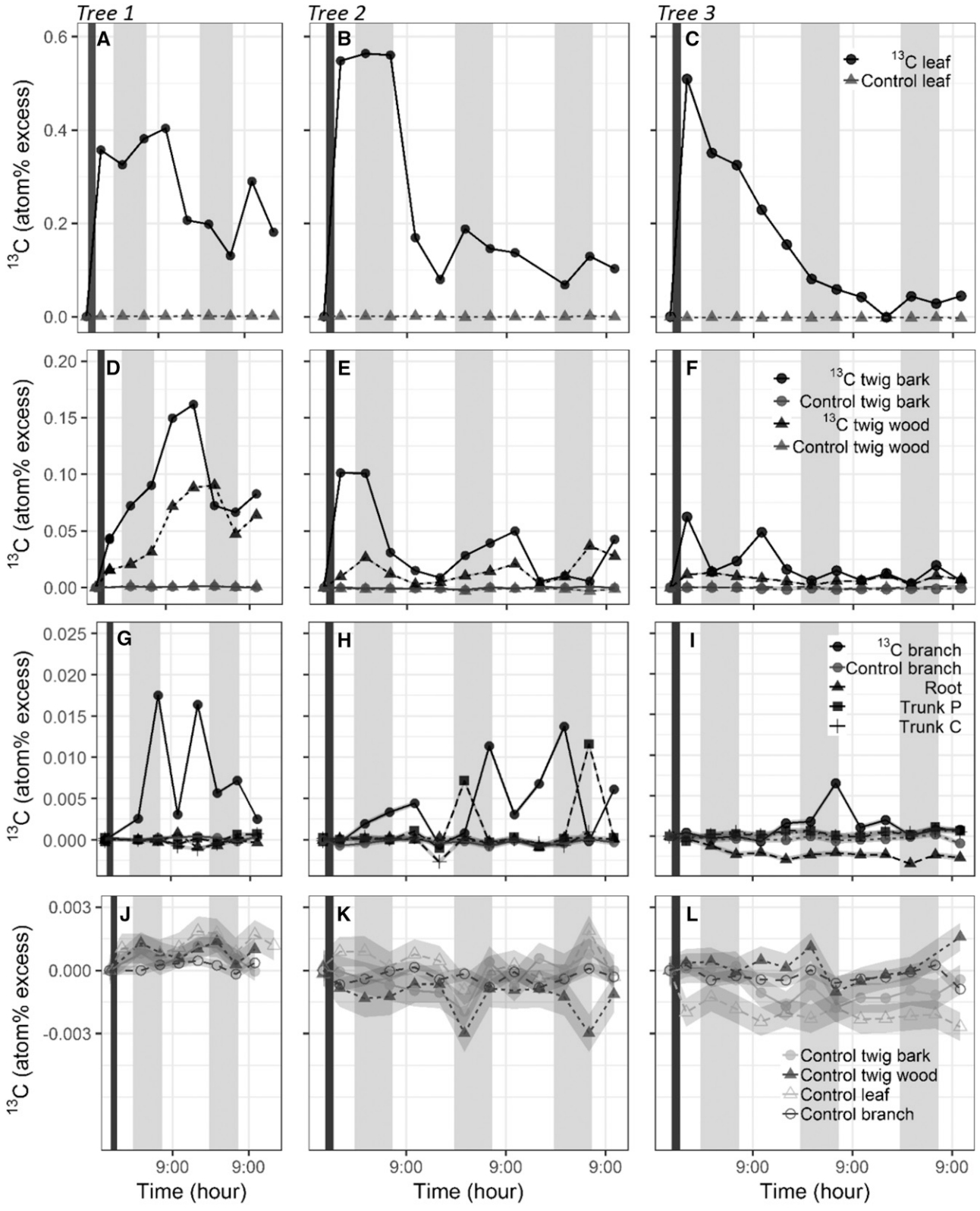

Figure 5. Diurnal dynamics of NSC allocation in the overall architecture of the tree over 3 d. Pulse labeling of ^{13}C was applied to a branch (branch ^{13}C) for 2 h (dark vertical bars) in tree 1 (A, D, G, and J), tree 2 (B, E, H, and K), and tree 3 (C, F, I, and L). Levels of ^{13}C were quantified in leaves (A–C), wood and bark of twigs (D–F), and wood at additional locations in the tree architecture, including trunk P and trunk C and in the roots (G–I). ^{13}C atomic percent was compared with initial values to calculate APE. APE

Short-Term Allocation of Newly Photosynthesized Sugars

Using in situ labeling, we show that newly assimilated $^{13}CO_2$ can be found in the woody tissue of twigs within 2 h after labeling. In leaves, the increase of APE after labeling was followed by a steady decrease reflecting NSC mobilization via respiration and their dilution by newly assimilated nonlabeled CO_2. This drop in APE also is likely due to basipetal translocation, as evidenced by the increase of APE in twigs and branches hours after APE increased in leaves (Fig. 5). It has been shown that night-respired CO_2 from leaves comes from the mixture of current NSC assimilated during the day and older stored NSC (Nogués et al., 2006). Since starch levels reach a nearly null value at dawn in leaves, other potential NSC sources to support nighttime respiration could include NSC imported from neighboring twigs (Fig. 1). The unexpected increase of APE in leaves over the following days is in line with the idea that NSC return from neighboring storage organs (Fig. 5; Supplemental Fig. S3). While the interpretation that this increase is due to noise from sampling a material with a high range of APE values cannot be ruled out, we think our consistent localized sampling mitigates potential noise. Furthermore, the frequency and magnitude of APE increases are beyond what can be attributed to sampling noise. Similarly, CO_2 respired in woody tissues and dissolved in the sap could be reassimilated in the leaves and contribute to the APE increase (Teskey et al., 2008). Future efforts should demonstrate the significance of the xylem sap contribution to leaf carbon budget.

A potential explanation for the observed return of labeled NSC to leaves could be that twigs provide alternative carbon sources at the end of the night, when starch pools are depleted. As *Prunus* trees have passive phloem loading, decreasing leaf SC concentration could lead to a reduction in phloem export rate and potentially explain the discrepancy between herbaceous and perennial starch-sugar ratios in leaves (Fig. 1; Turgeon, 2010; Jensen et al., 2012). Twig phloem loading at night would ensure a steady phloem flow. When comparing the results from the NSC diurnal trends and ^{13}C allocation, the increase in NSC concentration did not coincide with an increase in APE, suggesting that a high rate of NSC accumulation in a storage compartment is not necessarily the result of recent assimilate allocation but probably a more general retranslocation of NSC. For instance, while twigs tended to increase NSC storage at night, an increase of APE was not observed during the night following the pulse event (Figs. 2 and 5). Yet, since these two experiments were not performed at the same time during the summer, future studies should validate that the influx of NSC originates from lower organs. The return of labeled carbon in woody tissues points toward the presence of vertical mixing and highlights the necessity to shift the study of tree NSC to a more process-oriented approach that emphasizes NSC fluxes, as advocated by Hartmann and Trumbore (2016).

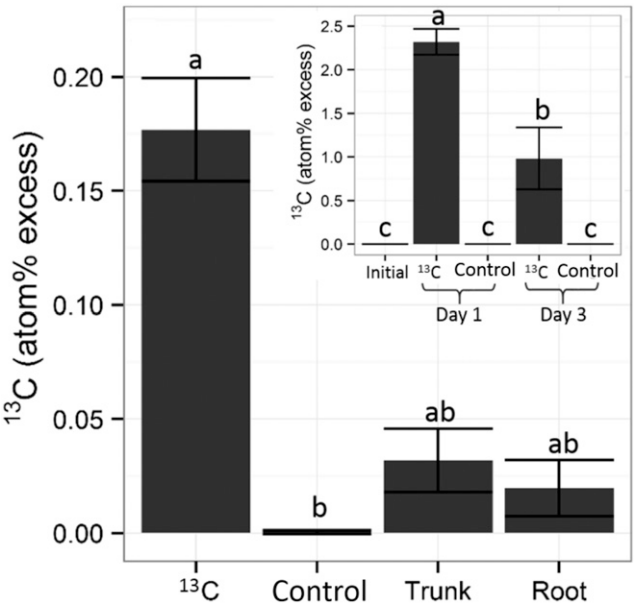

Figure 6. ^{13}C allocation pattern on day 3 after treatment of one bagged branch with $^{13}CO_2$ in 2-year-old potted almond trees. The within-tree spatial distribution of ^{13}C in the wood of ^{13}C twig (^{13}C), control twig (Control), trunk, and roots is shown. Assimilation of ^{13}C occurred on day 1 in leaves of the bagged branch, and translocation was observed on day 3 (inset). Samples were harvested in the afternoon and dried immediately for ^{13}C content analysis. Data points represent mean values for three trees. Error bars represent SE. Letters represent significant groups within tissues according to Kruskal-Wallis and Tukey's honestly significant difference (HSD; inset) tests.

The return of NSC to leaves via upward phloem flux would imply quick changes in phloem direction, with upward flow from twigs followed by downward flow when leaves become photosynthetically active. Another explanation for the return of NSC to the leaves could be that some sugars flow with the transpiration stream. The phloem leakage-retrieval mechanism postulates that the phloem discharges sugars along its path to the apoplast (Knoblauch and van Bel, 1998; Knoblauch and Peters, 2010; De Schepper et al., 2013). Phloem has been shown to leak sugars to the apoplast, allowing for an accumulation of sugars in the xylem parenchyma cells and apoplast under low

Figure 5. (*Continued.*)
levels of the tissues from branch ^{13}C (leaves, twig wood and bark, and branch wood; black symbols) were compared with natural variation in tissues from adjacent control branches (J–L; gray symbols in A–I). Gray ribbons around data points represent the SD for natural abundance (too small to show for the scale of A–I). ^{13}C levels and variation observed in all of the branch tissues and in the trunk P exceeded natural variation. Shaded areas represent nighttime.

transpirational demand (Alves et al., 2007; Secchi and Zwieniecki, 2011; Tixier et al., 2017). Here, we observed an overnight accumulation of SC in xylem sap of up to ~1.7 mg mL^{-1} and a constant low level during the day at ~0.7 mg mL^{-1} (Fig. 4). The sudden drop from 1.7 to 0.7 mg mL^{-1} following sunrise most likely reflects the transport of accumulated sugars via the transpirational stream. These sugars would flow to transpiring leaves and explain the increase in ^{13}C APE (Fig. 7). The significance to the leaf carbon budget of these sugars transported by the transpirational stream can be estimated with simple calculations and comparison with instantaneous water use efficiency. Assuming that 400 water molecules are exchanged for one CO_2 during assimilation (instantaneous water use efficiency of 2.5 mmol CO_2 [mol water]$^{-1}$), the resulting carbon-to-water ratio is 0.0025 (Romero et al., 2004). In the sap, a sugar concentration of 1.7 mg mL^{-1} has 0.2 mmol of Glc equivalent for 1 mol of water, generating a carbon-to-water ratio of 0.001. Thus, morning stream sap can constitute up to 29% of leaf carbon intake. Later in the day, when sap sugar concentration decreases (0.6 mg mL^{-1}), this value would drop but still could contribute up to ~13% of carbon uptake. The proposed transpiration-driven transport of sugars allows for secondary equilibration and redistribution of sugars, as observed previously during the spring in walnut (*Juglans regia*) trees (Tixier et al., 2017).

The results presented in Figures 5 and 6 provide evidence that the assimilated ^{13}C was allocated basipetally, with the dispersion of photosynthates occurring along the phloem, in the branch, trunk, and root storage pools, while no detectable allocation to neighboring control branches was observed. Similarly, in smaller trees 3 d after the labeling events, ^{13}C was detected in the labeled twig, trunk, and root but not in the adjacent

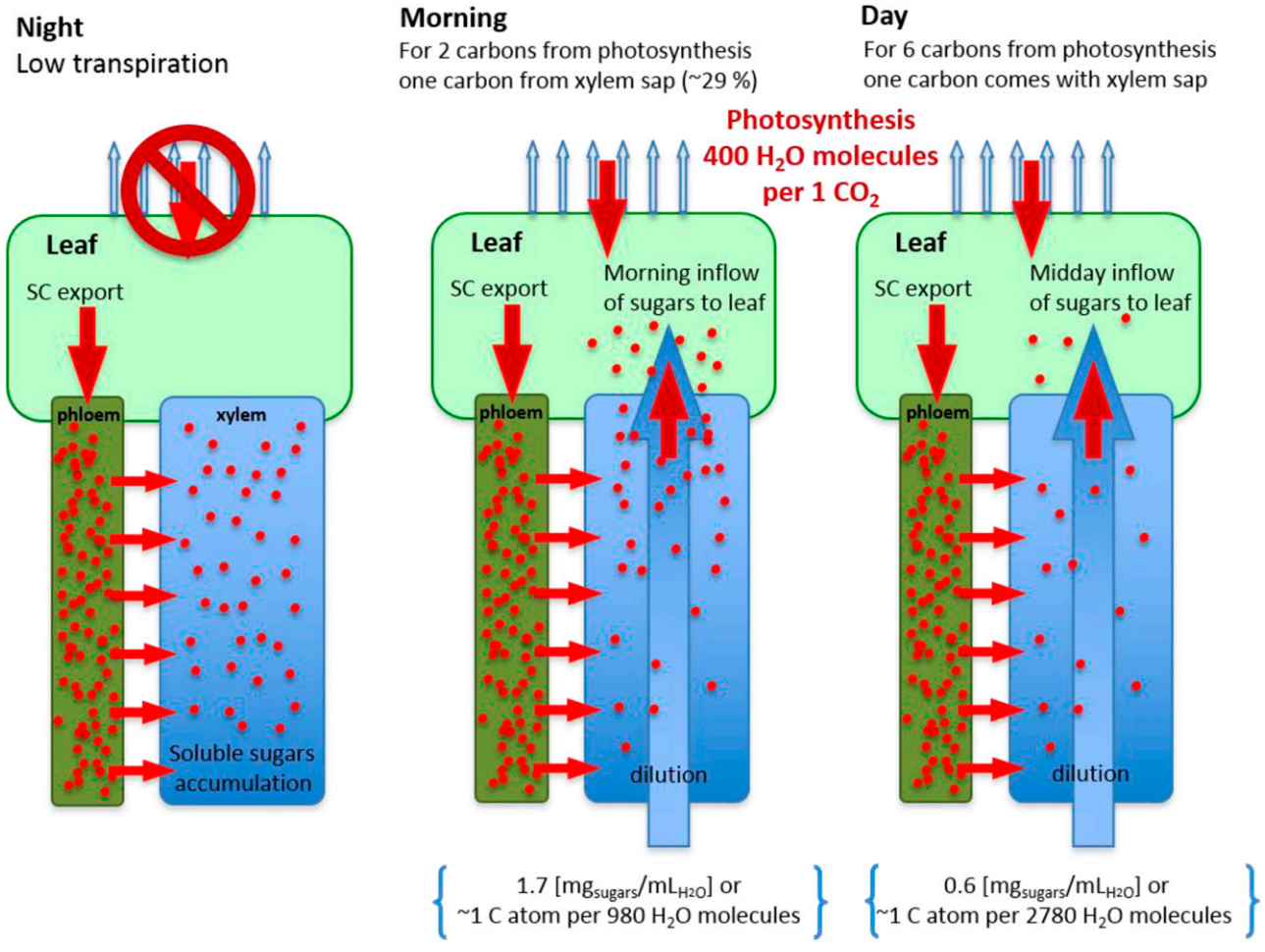

Figure 7. Proposed hypothesis that xylem offers a secondary pathway for sugar redistribution. Phloem leaks sugars to the apoplast, allowing for sugar accumulation in the xylem parenchyma cells and apoplast under low transpirational demand at night, which leads to overnight accumulation of SC in xylem sap of up to ~2 mg mL^{-1}. The sudden drop from 2 to 0.7 mg mL^{-1} following sunrise is due mostly to the transport of accumulated sugars via the transpirational stream to leaves. Assuming that 400 water molecules are exchanged for one CO_2 molecule during assimilation, the resulting carbon-to-water ratio is 0.0025. In the sap, the sugar concentration of 2 mg mL^{-1} generates a carbon-to-water ratio of 0.0012. Thus, morning stream sap can constitute up to 29% of leaf carbon intake. During the day, this value would drop but still could contribute up to ~13% of carbon uptake.

control twig (Fig. 6). Older parts of the trees, including branch wood, trunk, and roots, showed small to moderate delayed changes in ^{13}C APE that were most likely the effect of distance and local NSC pool size. The absence of an APE increase in the adjacent control branches provides evidence for branch autonomy during the growing season (Lacointe et al., 2004). The lack of APE increase in control shoots also can be explained by the fact that the pulse event was relatively short and diluted successively in the storage compartment, as observed in Figure 5. Consequently, as xylem sugars only constitute less than 0.1% of total carbon, detection of the pulse labeling event would be very difficult. In addition, lack of ^{13}C detection might be related to the level of xylem sectoriality (Zanne et al., 2006). The rapid rate of dispersion of recent assimilates through the entire canopy argues against the idea that storage replenishment during the growing season occurs from top to bottom or bottom to top (Fig. 5). Rather, our results suggest that trees fill the storage uniformly across the entire organism, with a high level of continuous fluxes equalizing access to new photosynthates for all storage tissue.

CONCLUSION

This detailed study of diurnal NSC dynamics provides a basis and time scale to address local mixing processes of storage in trees. We find evidence of the presence of vertical mixing at short time scales (hours to days) and argue for a paradigm shift in the study of tree NSC dynamics, which are currently seen as slow invariable reserves. We highlight the need for further studies that integrate a holistic understanding of the spatial and temporal diversity of NSC storage pools. The major role that roots might play as an NSC source under conditions of limited CO_2 assimilation also deserves more attention. Furthermore, the effects of environmental conditions and phenology on NSC levels in conjunction with diurnal variation should be addressed in the future (Supplemental Fig. S4). We observe that, in the short term, NSC are dispersed throughout the entire canopy, suggesting that storage replenishment during the growing season occurs in a synchronous/equalized pattern in different organs. Considering the high degree of NSC variation at the diurnal scale, future studies should sample at different positions in the canopy and avoid generalizing from the observation of storage in one location to the overall tree. Second, the proposed hypothesis that the xylem constitutes a secondary pathway for sugar redistribution offers exciting perspectives. It suggests a mechanism to explain NSC redistribution and the mechanism responsible for the equalization of sugar content across the tree architecture (Fig. 7). Furthermore, the presence of sugars in the transpiration stream can influence water transport in leaves via sugar sensing through hexokinase and aquaporins (Kelly et al., 2017). Finally, the vertical upward supply of carbohydrates could sustain phloem flow in passive loaders and provide metabolites for respiration when leaf NSC reserves are being depleted at the end of the night (Turgeon, 2010).

MATERIALS AND METHODS

Diurnal NSC Dynamics Analysis

Plant Material and Sample Collection

Diurnal NSC dynamics were investigated on five 7-year-old (~20 cm diameter at breast height and ~6 m height), well-watered, healthy almond (*Prunus dulcis*) trees grown in an orchard at the University of California, Davis (38.542154° N, 121.796485° W), on September 10, 2015. Over a period of 24 h, tissue samples were collected every 4 h at 5:00, 9:00, 13:00, 17:00, 21:00, and 1:00. To compare potential differences between days, we collected additional samples at 13:00 the next day. Environmental data over the period of sample collection were recorded (Supplemental Fig. S5). Photosynthetically mature leaves, current year twigs, 2-cm-long wood cores from 5-year-old branches, 4-cm-long wood cores from the trunk, and samples from structural coarse roots and small active roots were harvested for NSC analysis. Bark (including phloem and cambium) was removed from sapwood core samples; trunk cores were separated further into trunk P and trunk C. After collection, samples were quickly (within 10 min) brought to the laboratory, bark (including phloem and cambium) was stripped from the wood of twigs, and samples were immediately (within 1 min) placed at 75°C. In addition, 100-cm-long 2-year-old branches were harvested for xylem sap collection. Once cut, branches were placed immediately in a large plastic bag containing wet tissue paper to retain moisture prior to sap extraction.

Sap Collection and Carbohydrate Analysis

Xylem sap collection was performed using vacuum suction (Secchi and Zwieniecki, 2012). In short, branches were fixed to a small vacuum chamber containing a collection tube. After applying suction to the chamber, the branch was cut successively to allow vessel opening for sap aspiration starting at the farthest point from the chamber to the closest. Approximately 1 mL of sap was collected from each branch. Prior to analysis, sap samples were kept at −20°C.

After sample collection, NSC samples were dried at 75°C for 48 h. Then, to measure SC and starch, they were ground into a fine and homogenous powder using a ball mill. SC were extracted by incubating 25 mg of dry material in 1 mL of deionized water for 15 min at 70°C followed by centrifugation (10 min at 21,000*g*). The supernatant was diluted 1:20, and SC were quantified using anthrone as a reagent (0.1% [m/v] in 98% [v/v] sulfuric acid) by reading A_{620} (Leyva et al., 2008). The remaining pellet was kept for starch analysis. The pellet was washed two times with 80% (v/v) ethanol, incubated 10 min at 100°C to allow starch gelatinization, and then digested with 0.7 units of amylase and 7 units of amyloglucosidase in an acetate buffer (pH 5.5) for 4 h at 37°C. Once the digestion was finished, samples were centrifuged for 5 min at 21,000*g*. The supernatant was diluted 1:20 and quantified using the same method described above (Tixier et al., 2017).

As an alternative to destructive harvests, the biomasses of the trunk, branches, and twigs of a 7-year-old almond tree were calculated using the L-Almond model and used to estimate tree-level NSC content (Da Silva et al., 2014). This heuristic approach provided quantitative values for pools and fluxes. The L-Almond model is a functional-structural model based on the L-Peach model, which uses carbon and water exchanges to simulate the development and growth of almond trees. Since the L-Almond model does not model root biomass, it was estimated from a root:shoot ratio of 1:5 according to the literature (Harris, 1992). The products of the measured NSC concentrations and modeled biomass for each organ were calculated to estimate the NSC content for each organ.

Temporal Allocation of Newly Photosynthesized Compounds Derived from $^{13}CO_2$ Pulse Labeling

An isotope-labeling experiment was conducted in the same orchard as described above on June 17, 2016. Three large, 4-m-long branches (~5 years old) from three different trees were placed in translucent plastic bags (~2,000 L) while still attached to the tree at 14:00, and pulses of $^{13}CO_2$ (99 Atom % ^{13}C;

Sigma-Aldrich) were injected into the bag for 2 h using a syringe to maintain a continuous level of CO_2 (~300 ppm) in the bag. CO_2 levels were monitored using a LiCor 6400, air in the bag was mixed with a battery-powered electric fan, and the bags were removed after 2 h. Despite underestimating the levels of CO_2 because the infrared gas analyze (IRGA) O_2 analyzer has a lower sensitivity to $^{13}CO_2$ (one-third detection), LiCor monitoring ensured that a minimum of 300 μL L^{-1} CO_2 was consistently present for assimilation in the three bags (McDermitt et al., 1993). Following the initial collection of samples at 13:00 prior to $^{13}CO_2$ exposure, consecutive sampling was conducted every 6 h (17:00, 23:00, 5:00, and 11:00) for 3 d, with sunrise being at 6:00 and sunset at 21:00. Environmental data over the period of sample collection were recorded (Supplemental Fig. S1). Photosynthetically mature leaves, current-year twigs, and 2-cm-long wood cores from 5-year-old branches were harvested from both branches subjected to $^{13}CO_2$ and similarly sized adjacent control branches located across the crown. Four-centimeter-long cores from the trunk in addition to coarse roots were sampled at the same time. Residual bark was removed from the sampled cores. Trunk cores were separated into trunk P and trunk C. After collection, samples were quickly brought to the laboratory (within 10 min), bark was stripped from the wood of the twigs, and all samples were immediately placed at 75°C for 48 h.

Samples of leaves, bark, wood, and roots were ground into a fine and homogenous powder using a ball mill for isotopic analysis to calculate the amount and allocation of newly photosynthesized carbon derived from the $^{13}CO_2$ pulse. Measurements of ^{13}C were conducted using an Elementar Vario EL Cube or Micro Cube elemental analyzer (Elementar Analysensysteme) interfaced to a PDZ Europa 20-20 isotope ratio mass spectrometer (Sercon) at the Stable Isotope Facility of the University of California, Davis. The uptake and allocation of labeled carbon was expressed as ^{13}C APE, which corresponds to the difference between the absolute abundance of isotope in terms of atomic percent (^{13}C atomic percent) in samples and the initial ^{13}C atomic percent baseline values determined for each plant and tissue before the labeling event following the equation (Fisher et al., 1979):

$$\mathrm{APE} = \mathrm{Atom\%}^{13}\mathrm{C}_{\mathrm{sample}} - \mathrm{Atom\%}^{13}\mathrm{C}_{\mathrm{baseline}}$$

where:

$$\mathrm{Atom\%}^{13}\mathrm{C} = \left({}^{13}\mathrm{C} \Big/ \left({}^{13}\mathrm{C} + {}^{12}\mathrm{C}\right)\right) \times 100$$

A similar experiment was conducted on small 2-year-old potted almond trees on July 25, 2017 ($n = 3$). One branch per tree was placed in a translucent plastic bag and exposed to $^{13}CO_2$ pulses for 2 h from 14:00 to 16:00, maintaining a continuous ~300 CO_2 μL L^{-1} (see above). Leaves were collected before and after labeling events (day 1) and 2 d after (day 3) at 17:00, with sunrise being at 6:03 and sunset at 20:23. On day 3, trees were destructively sampled for root, trunk, and stem tissue from labeled and control twigs. Following collection, samples were processed to measure the uptake and allocation of ^{13}C with the same methods described above. Environmental data during sample collection were recorded (Supplemental Fig. S5).

Statistical Analysis

Diurnal NSC dynamics for all tissues were analyzed with nonlinear mixed-effects models, with time as a fixed effect and tree as a random effect, which accounted for the nonindependence of repeated measures of individual trees (using the nlme package; R Core Team, 2013) following the methods described by Pinheiro and Bates (2000). The time (t) effect was modeled as the sine-cosine function:

$$[\mathrm{NSC}] = \mathrm{a} + \mathrm{b}\,\sin(\mathrm{P} + \omega_1 \mathrm{t}) + \mathrm{c}\,\cos(\mathrm{P} + \omega_2 \mathrm{t}) + \varepsilon_{\mathrm{ij}}$$

where a, b, c, P, ω_1, and ω_2 were parameters optimized by nlme representing intercept (a), amplitude (b and c), phase (P), and frequency (ω_1 and ω_2) of the sinusoidal function. The absence of empirically significant autocorrelation in the repeated measurements was ensured using the ACF.lme function ($\alpha \leq 0.05$, nlme package; R Core Team, 2013). The nonlinear effect of time on NSC and model parsimony was assessed by model comparison following an information theoretic approach, using Akaike's information criterion (Akaike, 1974). ANOVA was then performed on each model ($\alpha \leq 0.05$), and Tukey's HSD tests were performed to separate means. Data from the saplings experiment were analyzed with ANOVA considering fixed effects, and Tukey's HSD tests were performed to separate means. Nonparametric data from the inset in Figure 6 were analyzed with Kruskal-Wallis and multiple comparisons (Siegel and Castellan, 1988).

Supplemental Data

The following supplemental materials are available.

Supplemental Figure S1. Diurnal NSC trends in bark.

Supplemental Figure S2. Diurnal dynamics of total NSC content in the tree.

Supplemental Figure S3. Diurnal dynamics of APE in leaves of 1-year-old saplings of almond.

Supplemental Figure S4. Leaf diurnal dynamics of starch concentration in June 2016.

Supplemental Figure S5. Environmental conditions during field experiments.

ACKNOWLEDGMENTS

We are grateful for help from Paula Delgado Guzman, Jessie Godfrey, and Lu Zhang in the field. We thank the University of California, Davis, stable isotope facility for isotope analysis. We thank Guillaume Théroux-Rancourt and Pauline Maillard for advice on statistical analysis and Jessie Godfrey and Matthew Gilbert for comments on the article.

Received July 31, 2018; accepted October 18, 2018; published October 29, 2018.

LITERATURE CITED

Akaike H (1974) A new look at statistical model identification. IEEE Trans Automat Contr **19:** 716–723

Alves G, Decourteix M, Fleurat-Lessard P, Sakr S, Bonhomme M, Améglio T, Lacointe A, Julien JL, Petel G, Guilliot A (2007) Spatial activity and expression of plasma membrane H^+-ATPase in stem xylem of walnut during dormancy and growth resumption. Tree Physiol **27:** 1471–1480

Bucci SJ, Scholz FG, Goldstein G, Meinzer FC, Sternberg LDSL (2003) Dynamic changes in hydraulic conductivity in petioles of two savanna tree species: Factors and mechanisms contributing to the refilling of embolized vessels. Plant Cell Environ **26:** 1633–1645

Chaffey N, Cholewa E, Regan S, Sundberg B (2002) Secondary xylem development in Arabidopsis: a model for wood formation. Physiol Plant **114:** 594–600 11975734

Charrier G, Poirier M, Bonhomme M, Lacointe A, Améglio T (2013) Frost hardiness in walnut trees (Juglans regia L.): How to link physiology and modelling? Tree Physiol **33:** 1229–1241

Charrier G, Ngao J, Saudreau M, Améglio T (2015) Effects of environmental factors and management practices on microclimate, winter physiology, and frost resistance in trees. Front Plant Sci **6:** 259

Da Silva D, Qin L, DeBuse C, DeJong TM (2014) Measuring and modelling seasonal patterns of carbohydrate storage and mobilization in the trunks and root crowns of peach trees. Ann Bot **114:** 643–652 24674986

De Schepper V, De Swaef T, Bauweraerts I, Steppe K (2013) Phloem transport: A review of mechanisms and controls. J Exp Bot **64:** 4839–4850

Dietze MC, Sala A, Carbone MS, Czimczik CI, Mantooth JA, Richardson AD, Vargas R (2014) Nonstructural carbon in woody plants. Annu Rev Plant Biol **65:** 667–687

Fisher TR, Haines EB, Volk RJ (1979) A comment on the calculation of atom percent enrichment for stable isotopes. Limnol Oceanogr **24:** 593–595

Graf A, Smith AM (2011) Starch and the clock: The dark side of plant productivity. Trends Plant Sci **16:** 169–175

Hansen P (1967) ^{14}C-studies on apple trees. III. The influence of season on storage and mobilization of labelled compounds. Physiol Plant **20:** 1103–1111

Harris RW (1992) Root-shoot ratios. J Arboric **18:** 39–42

Hartmann H, Trumbore S (2016) Understanding the roles of nonstructural carbohydrates in forest trees: From what we can measure to what we want to know. New Phytol **211:** 386–403

Hartmann H, Ziegler W, Kolle O, Trumbore S (2013) Thirst beats hunger: Declining hydration during drought prevents carbon starvation in Norway spruce saplings. New Phytol **200:** 340–349

Hoch G, Richter A, Körner C (2003) Non-structural carbon compounds in temperate forest trees. Plant Cell Environ **26:** 1067–1081

Jensen KH, Mullendore DL, Holbrook NM, Bohr T, Knoblauch M, Bruus H (2012) Modeling the hydrodynamics of phloem sieve plates. Front Plant Sci **3:** 151

Keel SG, Siegwolf RTW, Körner C (2006) Canopy CO_2 enrichment permits tracing the fate of recently assimilated carbon in a mature deciduous forest. New Phytol **172:** 319–329

Keel SG, Siegwolf RTW, Jäggi M, Körner C (2007) Rapid mixing between old and new C pools in the canopy of mature forest trees. Plant Cell Environ **30:** 963–972

Kelly G, Sade N, Doron-Faigenboim A, Lerner S, Shatil-Cohen A, Yeselson Y, Egbaria A, Kottapalli J, Schaffer AA, Moshelion M, et al (2017) Sugar and hexokinase suppress expression of PIP aquaporins and reduce leaf hydraulics that preserves leaf water potential. Plant J **91:** 325–339

Knoblauch M, Peters WS (2010) Münch, morphology, microfluidics: Our structural problem with the phloem. Plant Cell Environ **33:** 1439–1452

Knoblauch M, van Bel JE (1998) Sieve tubes in action. Plant Cell **10:** 35–50

Lacointe A, Deleens E, Améglio T, Saint-Joanis B, Lelarge C, Vandame M, Song GC, Daudet FA (2004) Testing the branch autonomy theory: A $^{13}C/^{14}C$ double-labelling experiment on differentially shaded branches. Plant Cell Environ **27:** 1159–1168

Leyva A, Quintana A, Sánchez M, Rodríguez EN, Cremata J, Sánchez JC (2008) Rapid and sensitive anthrone-sulfuric acid assay in microplate format to quantify carbohydrate in biopharmaceutical products: Method development and validation. Biologicals **36:** 134–141

Loescher WH, McCamant T, Keller JD (1990) Carbohydrate reserves, translocation and storage in woody plant roots. HortScience **25:** 274–281

McDermitt DK, Welles JM, Eckles RD (1993) Effect of Temperature, Pressure and Water Vapor on Gas Phase Infrared Absorption by CO_2. LI-COR, Lincoln, NE

Muhr J, Messier C, Delagrange S, Trumbore S, Xu X, Hartmann H (2016) How fresh is maple syrup? Sugar maple trees mobilize carbon stored several years previously during early springtime sap-ascent. New Phytol **209:** 1410–1416

Nogués S, Damesin C, Tcherkez G, Maunoury F, Cornic G, Ghashghaie J (2006) $^{13}C/^{12}C$ isotope labelling to study leaf carbon respiration and allocation in twigs of field-grown beech trees. Rapid Commun Mass Spectrom **20:** 219–226

Norris CE, Quideau SA, Landhäusser SM, Bernard GM, Wasylishen RE (2012) Tracking stable isotope enrichment in tree seedlings with solid-state NMR spectroscopy. Sci Rep **2:** 719

Pinheiro JC, Bates DM (2000) Mixed-Effects Models in S and S-PLUS. Springer, New York

Pyl ET, Piques M, Ivakov A, Schulze W, Ishihara H, Stitt M, Sulpice R (2012) Metabolism and growth in Arabidopsis depend on the daytime temperature but are temperature-compensated against cool nights. Plant Cell **24:** 2443–2469

R Core Team (2013) R: A Language and Environment for Statistical Computing. R Foundation for Statistical Computing. http://www.r-project.org/.le

Regier N, Streb S, Zeeman SC, Frey B (2010) Seasonal changes in starch and sugar content of poplar (Populus deltoides × nigra cv. Dorskamp) and the impact of stem girdling on carbohydrate allocation to roots. Tree Physiol **30:** 979–987

Richardson AD, Carbone MS, Keenan TF, Czimczik CI, Hollinger DY, Murakami P, Schaberg PG, Xu X (2013) Seasonal dynamics and age of stemwood nonstructural carbohydrates in temperate forest trees. New Phytol **197:** 850–861

Richardson AD, Carbone MS, Huggett BA, Furze ME, Czimczik CI, Walker JC, Xu X, Schaberg PG, Murakami P (2015) Distribution and mixing of old and new nonstructural carbon in two temperate trees. New Phytol **206:** 590–597

Romero P, Navarro JM, García F, Botía Ordaz P (2004) Effects of regulated deficit irrigation during the pre-harvest period on gas exchange, leaf development and crop yield of mature almond trees. Tree Physiol **24:** 303–312

Sala A, Woodruff DR, Meinzer FC (2012) Carbon dynamics in trees: Feast or famine? Tree Physiol **32:** 764–775

Secchi F, Zwieniecki MA (2011) Sensing embolism in xylem vessels: the role of sucrose as a trigger for refilling. Plant Cell Environ **34:** 514–524

Secchi F, Zwieniecki MA (2012) Analysis of xylem sap from functional (nonembolized) and nonfunctional (embolized) vessels of *Populus nigra*: Chemistry of refilling. Plant Physiol **160:** 955–964

Siegel S, Castellan J (1988) Nonparametric Statistics for the Behavioural Sciences. McGraw-Hill, New York

Sperling O, Silva LCR, Tixier A, Théroux-Rancourt G, Zwieniecki MA (2017) Temperature gradients assist carbohydrate allocation within trees. Sci Rep **7:** 3265–3275

Stitt M, Zeeman SC (2012) Starch turnover: Pathways, regulation and role in growth. Curr Opin Plant Biol **15:** 282–292

Streb S, Zeeman SC (2012) Starch metabolism in Arabidopsis. The Arabidopsis Book **10:** e0160,

Teskey RO, Saveyn A, Steppe K, McGuire MA (2008) Origin, fate and significance of CO_2 in tree stems. New Phytol **177:** 17–32

Tixier A, Sperling O, Orozco J, Lampinen B, Amico Roxas A, Saa S, Earles JM, Zwieniecki MA (2017) Spring bud growth depends on sugar delivery by xylem and water recirculation by phloem Münch flow in Juglans regia. Planta **246:** 495–508

Turgeon R (2010) The role of phloem loading reconsidered. Plant Physiol **152:** 1817–1823

Wada H, Masumoto-Kubo C, Tsutsumi K, Nonami H, Tanaka F, Okada H, Erra-Balsells R, Hiraoka K, Nakashima T, Hakata M, et al (2017) Turgor-responsive starch phosphorylation in Oryza sativa stems: A primary event of starch degradation associated with grain-filling ability. PLoS ONE **12:** e0181272

Witt W, Sauter JJ (1994) Starch metabolism in poplar wood ray cells during spring mobilization and summer deposition. Physiol Plant **92:** 9–16

Woodruff DR, Meinzer FC, Marias DE, Sevanto S, Jenkins MW, McDowell NG (2015) Linking nonstructural carbohydrate dynamics to gas exchange and leaf hydraulic behavior in Pinus edulis and Juniperus monosperma. New Phytol **206:** 411–421

Zanne AE, Sweeney K, Sharma M, Orians CM (2006) Patterns and consequences of differential vascular sectoriality in 18 temperate tree and shrub species. Funct Ecol **20:** 200–206

Zeeman SC, Tiessen A, Pilling E, Kato KL, Donald AM, Smith AM (2002) Starch synthesis in Arabidopsis: Granule synthesis, composition, and structure. Plant Physiol **129:** 516–529